

RESEARCH PAPER

# Dielectric characterization using FEM modeling and ANNs for coaxial waveguide with conical open ended radiation

MOHAMED MOUNKID EL AFENDI<sup>1</sup>, MOHAMED TELLACHE<sup>1</sup>, JUNWU TAO<sup>2</sup>, BILAL HADJADI<sup>1</sup>  
AND MOUNCEF BENMIMOUNE<sup>3</sup>

*Since last decades, microwaves have received tremendous attention as an interesting tool for material characterization. In general, standard microwave measurement methods require cutting and polishing of samples to put it in a suitable waveguide or cavity. However, several methods have been developed in order to permit a non-destructive measurement. A well-known method is based on coaxial open-ended waveguide, which is used as a sensor for dielectric characterizations. Moreover, with the requirement of new forms, developing mathematical model for each one is not convenient. Indeed, the complex structures required in the industrial field can be perfectly designed with high-performance three-dimensional software. Many attempts have been done to solve the conversion problem by proposing different algorithms. Nevertheless, they are sensitive for complex structure that contains transition part. In this paper, we propose a dielectric measurement method based on the use of coaxial waveguide. A novel algorithm for dielectric characterization of complex structures is also presented, which is based on the joint use of artificial neuronal networks and finite element method. The proposed algorithm aims to find the dielectric characterization for complex structures. Experimental evaluations applied to solid and liquid dielectrics confirm the validation of the proposed algorithm.*

**Keywords:** Dielectric measurement, Coaxial open-ended waveguide, Finite element method, Radiation field, Neural networks

Received 7 September 2015; Revised 4 February 2016; Accepted 8 February 2016; first published online 8 March 2016

## I. INTRODUCTION

The interaction of microwave materials depends strongly on the electromagnetic proprieties. Many different methods have been elaborated for microwave measurement of materials and media properties. Generally, they are divided into two main groups: the first group is free-space methods, which is operating in the far-field region and employing horn antenna, whereas the second group, denoted waveguide methods, is operating in the near-field region and employing coaxial lines, waveguides, microstrip lines or cavity resonators as probe.

### A) Related work

The measurement of dielectric materials properties at radio-frequency has gained increasing importance, especially in research fields such as: material science, microwave circuit

design, absorber development, biological research, etc. Dielectric measurement is important, since it can provide the electrical or magnetic material characteristics, which is proved useful in many research and development fields [1, 2]. The dielectric properties can be measured by different methods, the following four methods are the more usefully: transmission/reflection (TR) line method [3], open-ended coaxial probe method [4], free-space method [5, 6], and resonant method [7].

Generally, the transition is a key part of the measurement methods, making possible the interconnection between different types of transmission lines. Hence, it is imperative to have a good characterization of these structures in order to assess their performance and provide information, which can be used during the design, measurement, or optimization processes. Moreover, it is worth to note that, the dielectric parameters are measured via the calculation of the transmission and reflection values, which are determined by means of a conversion method. In the literature, the most commonly conversion methods are: Nicolson–Ross–Weir method [8, 9], iterative method and non-iterative method [10], and short-circuit line (SCL) method [11].

Moreover, the conversion methods have been developed for a specific structure with analytic equations [12, 13]. However, the finite element method (FEM) can compute complex three-dimensional (3D) structure [14]. Consequently, an optimized model has been designing by using high-frequency structure

<sup>1</sup>Faculty of Electronics and Computers, University of Sciences and Technology Houari Boumediene, BP 32 El Alia, 16111 Bab Ezzouar, Algiers, Algeria. Phone: +213 558 77 10 45

<sup>2</sup>INPT-ENSEEIH, 2 rue Charles Camichel, BP 7122, 31071 Toulouse, Cedex 7, France

<sup>3</sup>Université du Québec à Montréal, 201, av. Président-Kennedy, Montreal, QC H2X 3Y7, Canada

**Corresponding author:**

M. El Afendi

Email: melafendi@usthb.z

simulator (HFSS). Thus, the experimental part is reduced to an elementary measurement. Nevertheless, a complex relationship for defining the dielectric material characteristic is required.

Recently, more focus has been given in this area by proposing different algorithms attempting to solve the dielectric characterization problem. Bartley *et al.* [15] have explored the use of artificial neuronal networks (ANNs) for coaxial open-end. The proposed approach has been successfully used to solve the analytic equation determination problem. Nevertheless, the ANNs have been trained using only real measurement samples, which decrease its performance due to the limitation of the generated training number. For further progress in capabilities, numerical method accuracy and hardware productivity, Eugene *et al.* [16] start using finite difference time domain (FDTD) software tool in order to reduce the cost achievement of simple rectangular waveguide structure. More recently, Acikgoz *et al.* [17] have investigated the use of Bayesian ANN algorithm. The latter leads to more improvement of dielectric characterization of materials. However, this proposal is sensitive to complex structures which contain transition part. Indeed, this form causes a shift between simulated and measured values.

## B) Contributions

In this paper, we propose a dielectric measurement system based on the use of coaxial waveguide. A non-standard coaxial cell with a conical transition and two coaxial probes are designed, which allows us to perform both permittivity and permeability measurement for large size of materials. In addition, we propose a new algorithm for the dielectric characterization of complex structures of dielectric. Firstly, the HFSS is used to generate the training database in order to design the conversion model, based on FEM. Secondly, in the operation phase, the ANN is used to estimate the dielectric parameters to test the materials through vector network analyzer (VNA) measured values. Moreover, due to the adaptation problem which appears when we deal with complex structure, another ANN is added in order to determine the correct values of dielectric characteristics. A crucial advantage of using ANN is that it allows the dielectric measurement of new complex materials. The proposed system is validated via simulation and experimental results.

## C) Organization

The rest of this paper is organized as follows. In the next section, we present the mathematical model of proposed system, based on FEM. In Section III, we build the 3D equivalent model of the adopted structure. The proposed conversion method based on ANN is presented in Section IV. Experimental results of the proposed system are presented in Section V. Finally, the conclusion and future work are provided in Section VI.

## II. MODELISATION AND SIMULATION

### A) Coaxial measurement model

In this section, the measurement model is built with two coaxial waveguides probes, where the measurement sample

is arranged between the fixing plates. The S-parameters are measured at the sample surface. The geometry model is illustrated in Fig. 1. The latter represents the reference model which has been used in [12], and explored in this paper for comparisons and evaluations purposes.

The boundary conditions are imposed at the border of the studied fields to ensure the uniqueness of the solution. The boundaries of the HFSS software calculation are defined by two conditions. The first one is about the radiation space which must be absorbed, whereas the second one concerns the walls of the coaxial waveguide and the plates, which have to be perfect conductors.

## B) Simulation

We consider a coaxial line, where the inner and outer radial dimensions are denoted by  $a$  and  $b$ , respectively. A metallic flange with  $c$  dimension is extended in the transverse direction and the tested object  $t$  must cover the waveguide aperture. The mentioned dimensions are selected to permit only the dominant TM mode propagation [13]. The Table 1 illustrates all system dimensions.

It is important to note that if only the transmission coefficient or the reflection coefficient is measured, either the complex permittivity or the complex permeability can be determined [12].

### 1) THE TRANSMISSION COEFFICIENT FOR DIFFERENT DIMENSIONS

The FEM method is used to determine the electromagnetic-field distribution in the sample of the aperture.

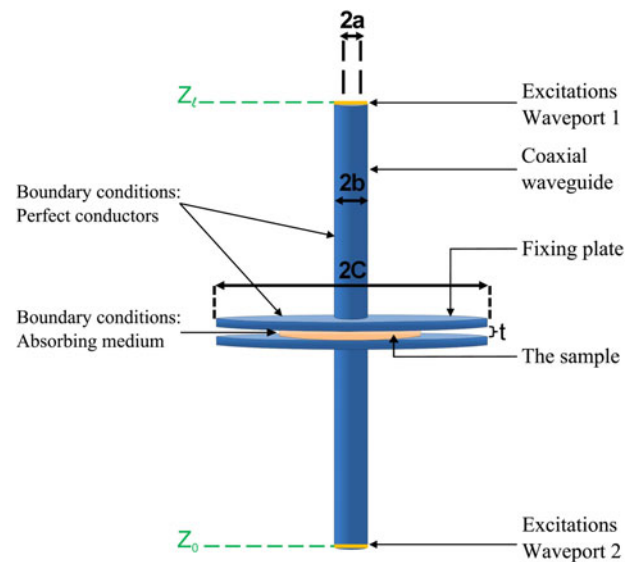


Fig. 1. Construction of the measurement model using HFSS.

Table 1. HFSS model parameters.

Parameter	Dimension
$2a$	3.04 mm
$2b$	7 mm
$c/b$	10
$t/b$	0.113–1.38

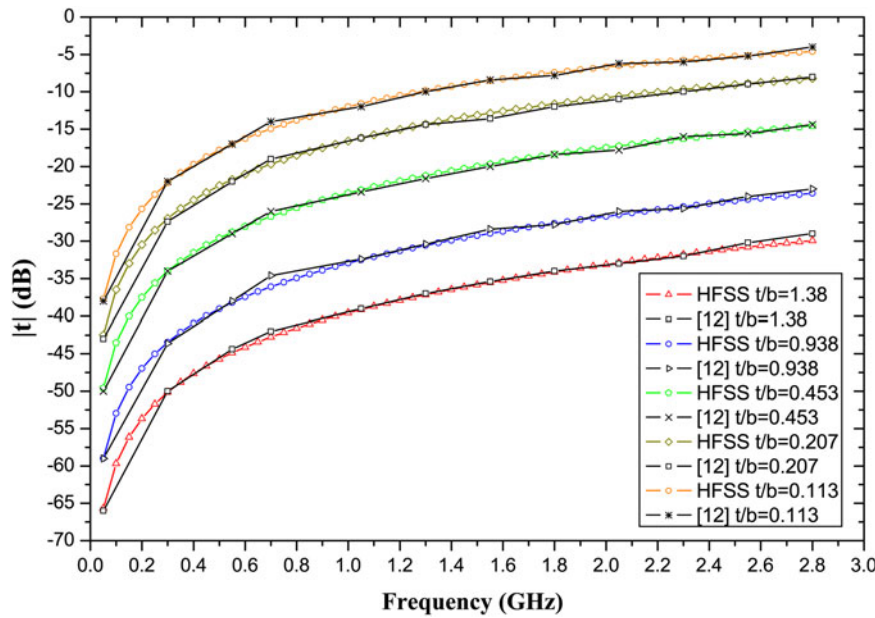


Fig. 2. Transmission coefficient comparison between the simulation and results presented in [12] for Tefflon.

Figure 2 shows the measurements of the transmission coefficient  $|\tau|$  as a function of the frequency. From the figure, we can clearly see a good agreement between our simulation and measurements for Tefflon. This comparison allows us to confirm the smooth functioning of our model. Also, we see from this figure that when the thickness  $t/b$  increases (i.e. from 0.113 to 1.38), the transmission coefficient becomes smaller.

The objective of this part is to validate the design of the considered model by comparing the obtained simulation results with those presented in [12]. Moreover, we show the effect of the variation of the sample dimension on the transmission coefficient. Since the variations of the reflection coefficient for the characterization of dielectric materials are less significant, in the proposed model, we illustrate only the transmission coefficient.

## 2) THE EFFECT OF MISALIGNMENTS ON THE TRANSMISSION COEFFICIENT FOR DIFFERENT RATIOS $T/B$

For a profound understanding of the variation effect of the ratio  $t/b$  on extracted parameters, we present the error caused by the coaxial probes misalignment. Note that a misalignment can be presented during the fixation of the two coaxial probes. In this study, the misalignment of the coaxial probes along the  $x$ -axis, which is perpendicular to the propagation direction of the TM mode in the waveguide, is investigated (see Fig. 3).

Using the 3D-simulation model in Fig. 1, the transmission coefficient considering misalignments distance, denoted by  $dx$ , is investigated. In Fig. 4, the transmission coefficient versus the frequency for different values of  $t/b$  is presented. In this simulation,  $dx$  worths 1 mm. From the obtained results it is obvious that the lowest misalignment errors are achieved for  $t/b$  which is equal to 0.938 and 1.38. However, according to Scott [12] the real and imaginary parts of the measured complex permittivities when  $t/b$  is equal to 0.938

and 1.38 are highly affected by the frequency variation. To guarantee a good compromise, we consider  $t/b$  equal to 0.453, since it offers both an accurate dielectric determination against the frequency variation and a latest misalignment error compared with the remaining  $t/b$  values.

## 3) THE TRANSMISSION COEFFICIENT FOR DIFFERENT MATERIALS

Once the model functionality confirmed, we began the characterization of wide range of materials.

The curves in Fig. 5 represent the variation of the transmission coefficient for different materials as a function of the frequency. In the simulation,  $t/b$  is equal to 0.453. As depicted in Fig. 5, the proposed model is able to well distinguish different

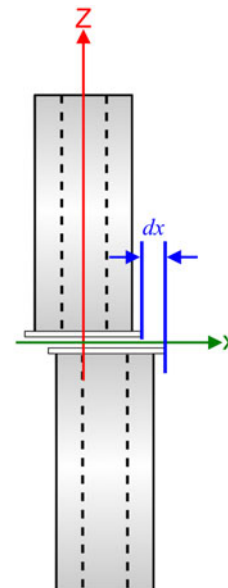


Fig. 3. Schematic representation of the performed misalignment plane.

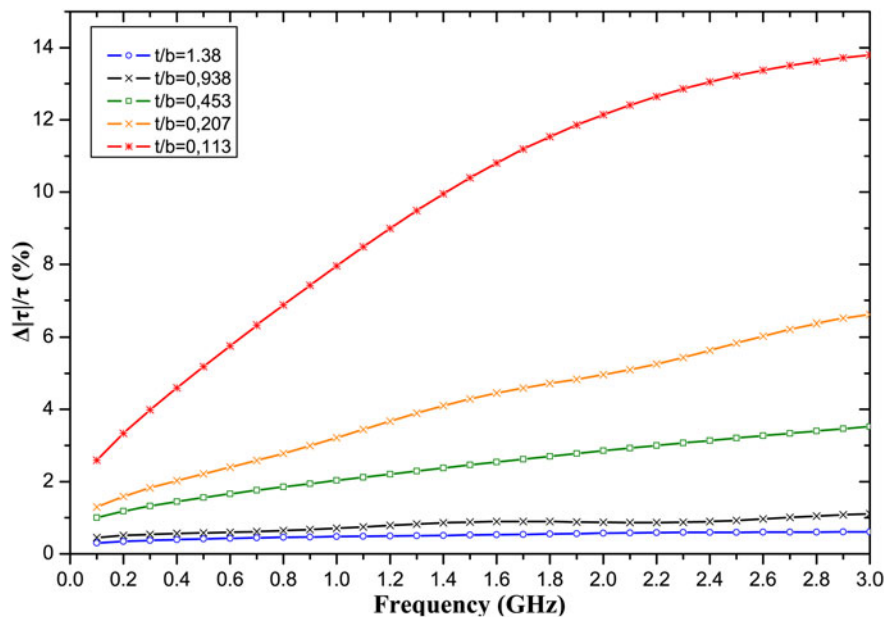


Fig. 4. Simulated transmission coefficient for Teflon, considering a misalignment  $dx = 1$  mm for different ratio  $t/b$ .

materials based on their transmission coefficients. As a result, we can note that the transmission coefficient can be used for dielectric characterization. However, the transmission coefficient is not efficient since it depends on other parameters such as thickness and used frequency, as presented in Fig. 2. Thus, an efficient characterization requires other independent parameters.

The objective of this part is to show the effect of the material samples on the transmission coefficient results for large non-destructive measurement.

4) STRUCTURE EVALUATION WITH AND WITHOUT TRANSITION

In Fig. 6, we present the simplified two schematics of the model, where different planes are used during the S-parameters

measurement. In the first representation, i.e. with transition (see Fig. 6(a)), the reference planes are at the coaxial waveguide connection. The latter takes on consideration the phase factor, which is equivalent to the distance between the sample surface and the connector plane, whereas in the second representation, i.e. without transition (see Fig. 6(b)), the reference planes are at the material under test. This is can be realized by involving the de-embedding function of the HFSS. Indeed, using the de-embedding, the influence of the transition on the actual material measurement can be cancelled out.

In Fig. 7, we present the curves of the simulated model with and without transition as a function of frequency for a variety of dielectric. These results permit to see the transition effect on the measurement of the transmission coefficient for different dielectric samples.

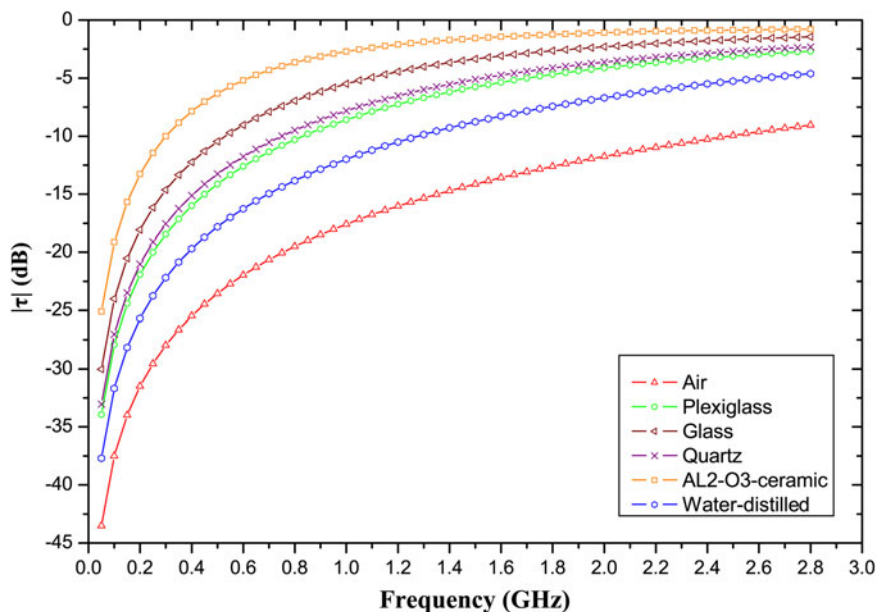


Fig. 5. Transmission coefficient comparison versus frequency for different materials with  $t/b = 0.453$ .



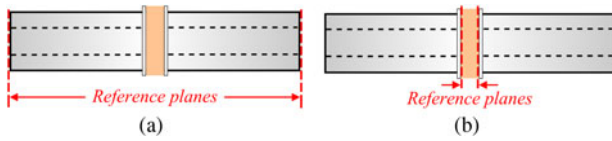


Fig. 6. Schematic representation of the performed two-planes in simulation.

Also, this study includes several dielectric materials in order to find good matching levels within the operating bandwidth. From the figure, we can deduce that for both methods (i.e. with and without transition) the transmittance is highly affected by the frequency. Indeed, the main source of errors is provided by the phase uncertainties about 0.75 GHz. For frequencies about 0.5 GHz, the transition has no effect on the measurement of the transmission

coefficient. It is important to note that the line impedance is adapted to 50  $\Omega$ .

### III. CONVERSION METHOD USING ANNS BASED ON FEM PREDICTION

Generally, the conversion of  $S$ -parameters to complex dielectric values is determined by solving the system of non-linear equations, according to the structure form. However, with the high requirement of new forms, developing mathematical model for each form is complicated. In addition, high-performance 3D software leads to design more complex structure. Nevertheless, these softwares require a numeric conversion method in order to define the dielectric material characteristics. Thus, we propose a novel algorithm based

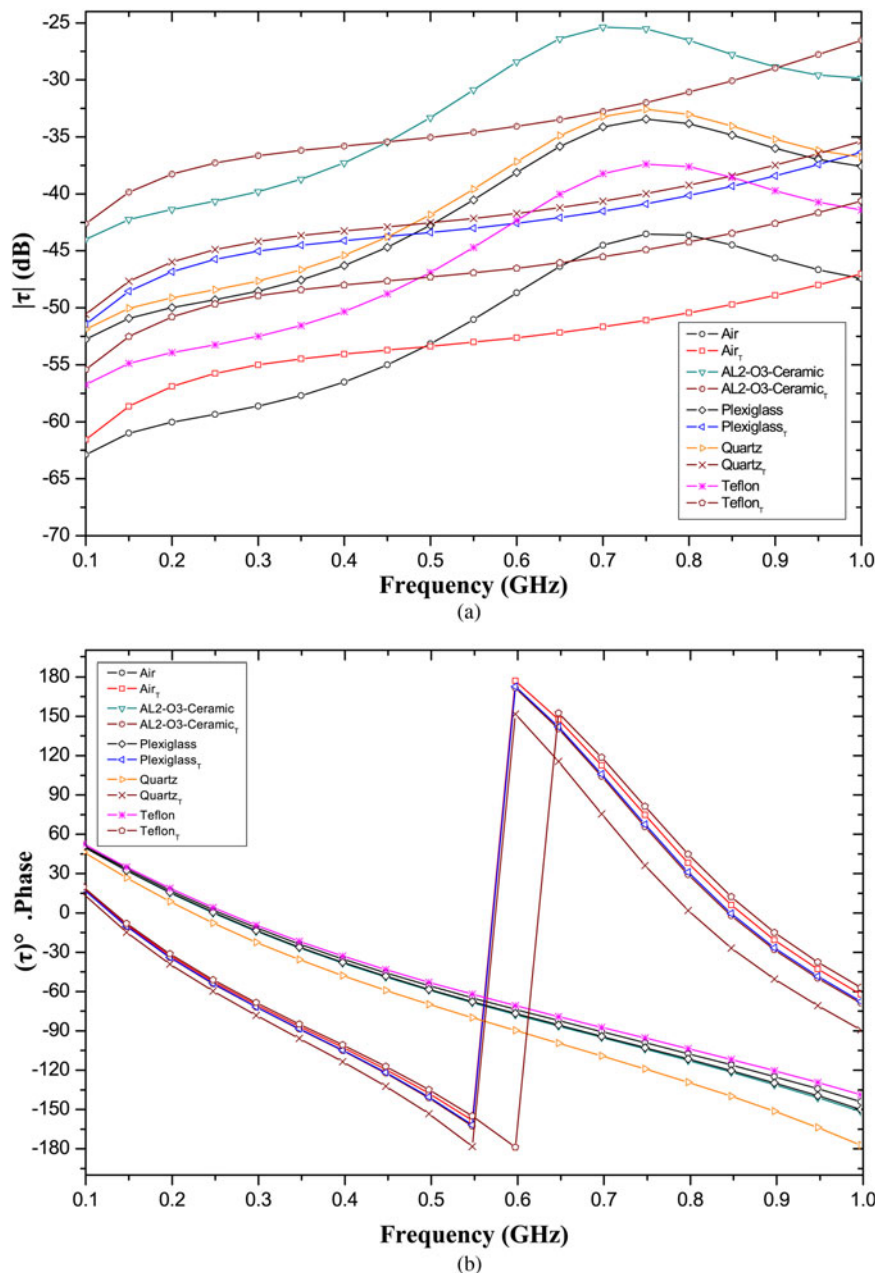


Fig. 7. Transmission coefficient of the structure with and without transition for different dielectric: (a) magnitude and (b) phase.

on the joint use of HFSS and ANN for frequency reference of 1 GHz and 10 mm of sample length.

### A) The design of the conversion method

In this study, using the HFSS, all experiments have been done under the following settings: Frequency is 1 GHz, the maximum number of passes worth 20, the maximum  $\Delta S = 0.01$  and the discrete type of sweep from 0.045 to 1 GHz with step of 0.002 GHz.

An ANN is applied to provide a conversion model for mapping S-parameters as input to dielectric characteristics as output. More precisely, the ANN is fed by the transmission coefficient module/phase ( $|\tau|$ ,  $\tau_\theta$ ) and reflections coefficient module/phase ( $|\rho|$ ,  $\rho_\theta$ ), resumed by  $x$  as input vector as well as the permittivity ( $\epsilon'_r$ ) and loss factor ( $\epsilon''_r$ ), resumed by  $\hat{Y}$  as output vector.

$$x = (|\tau|, \tau_\theta, |\rho|, \rho_\theta), \quad (1)$$

$$\hat{Y} = (\epsilon'_r, \epsilon''_r). \quad (2)$$

The architecture of the ANNs converter (see Fig. 8(b)) is consisting of four nodes as input, one hidden layer and two nodes as output.

Moreover, it is important to reveal that, the ANN converter requires high number of training samples in order to cover the whole permittivity material band. However, the procedure of providing real measurements is very expensive and long time is needed while preparing the measurement samples. Thus, we explore the simulation data for designing the training model.

In order to train the ANNs converter, the training database is generated by varying permittivity  $\epsilon'_r$  and loss factor  $\epsilon''_r$ , from 1 to 81 and  $10^{-5}$  to 0, respectively, to yield 2198 samples. Once the ANN is trained, it is able to determine the permittivity and loss factor.

In the ANNs converter, the training phase is performed using simulated samples, whereas in the operation phase the measured values are used. However, those latter are shifted from the simulated values due to the transition part.

Moreover, during the experiment phase we found that, the gap between simulated and measured transmission coefficient depends on the material under test. In other word, this difference is related to the S-parameters values. Hence, we have introduced an ANNs corrector (as depicted in Fig. 8(a)) in order to determine the corrected S-parameters from the obtained measured values more intelligently, according to the input features. Therefore, the ANNs corrector is adapted to the material under test.

The ANN corrector model is designed using only 20 measurement samples for training, which is very small against the simulated ones.

As a result, the proposed algorithm relies on the use of two ANNs: the first one uses the VNA measured data leading to correct the shift caused by the adaptation, presented in the complex structure, whereas, the second one is fed from the first ANNs to predict the dielectric characterization.

The advantages of the proposed ANNs corrector are: (i) reducing the shift in the transmission measurement, caused by the adaptation problem in the transition part; (ii) increasing the conversion accuracy using simulation and measurement data; (iii) taking into account the measured attenuation.

In this study, the training phase is performed considering two reference planes. Therefore, the proposed system is able to work whatever the chosen reference plane.

## IV. EXPERIMENTAL RESULTS

The broadband measurements of complex dielectric constants are required for several applications. Due to their relative simplicity, the TR method is widely used for measurement techniques. In this method, a sample is placed in a section of conical waveguide with large open end and the S-parameters are measured by a VNA. The measured S-parameters are related to the permittivity and permeability of the material by the relevant scattering equations. For the TR method, the system of equations that represent the model contains various variables, such as the permittivity, permeability, the reference plane position, the sample thickness, and the frequency. In the TR method, we have more data than the SCL method, since we have all the S-parameters. The system of

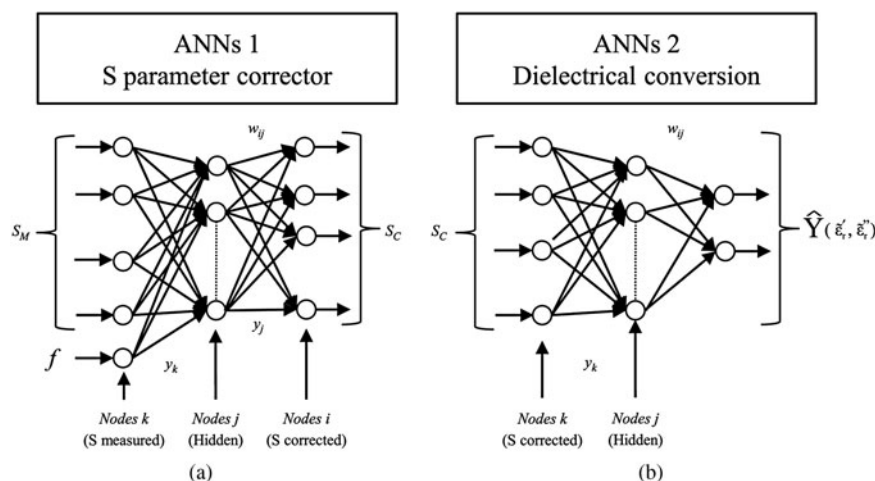


Fig. 8. Neural networks architecture: (a) corrector part and (b) conversion part.

equations is generally overdetermined and therefore can be solved using ANN algorithm.

### A) The tester

The brass coaxial waveguide is used for dielectric measurement, where a Teflon sample of 10 mm is placed on the probes section, which is connected to the VNA (ANRITSU 370). A calibration step for flexible cables and probes is performed in order to achieve more efficient results. In the first step, a short, open, load (SOLT) calibration with a standard  $N$  kit is applied. The systematic errors caused by the connector cables up to the reference plane are removed. In the second step, a TR calibration of the probs up to the measurement plane is performed. For more details about the calibration we refer to [18]. The calibration tester allows us to estimate the change in transmission loss with frequency. It also allows us to see the influence of the sample size on the measure.

#### 1) COAXIAL WAVEGUIDE WITH CONICAL APERTURE

In this paper, the optimized probes, which fit with this study, are presented in Fig. 9. This model differs from the model depicted in Fig. 1 by the fact that it contains a conical form, which allows a large dimension of material characterization. Note that the model has been designed under input impedance of  $50 \Omega$  with attenuation that depends on the frequency and the material under test. This attenuation is caused by the

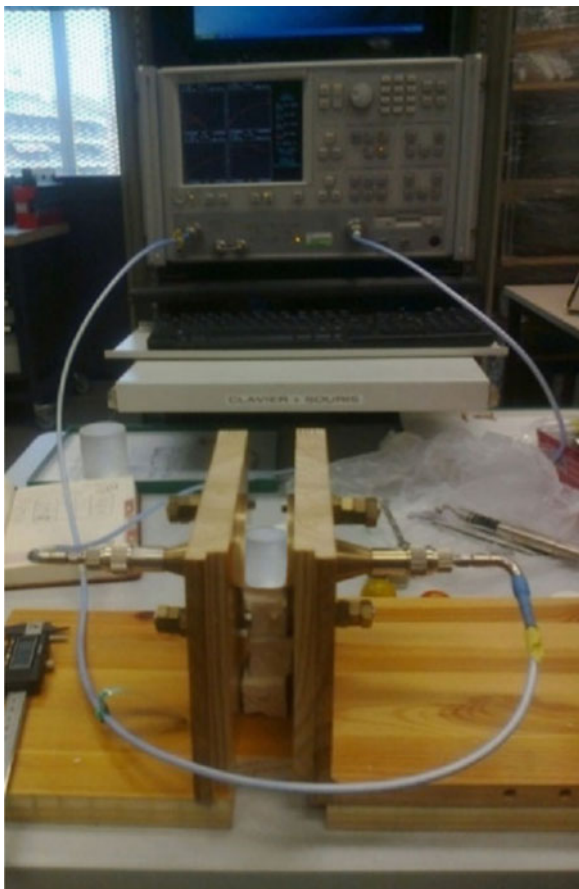


Fig. 9. The measurement tester used in the experiments, highlighting: VNA, Teflon (sample), and coaxial probes.

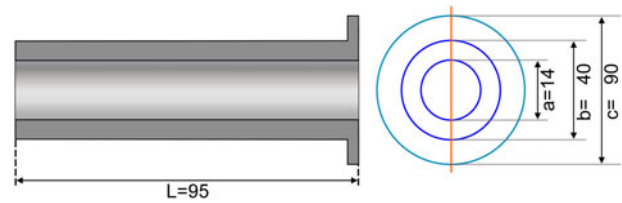


Fig. 10. Equivalent geometry of coaxial line model (mm).

conical form at the open-end of the coaxial waveguide. In additions, the structure dimension as shows in Fig. 10 is presented. This figure (i.e. Fig. 10) is a simplified scheme of Fig. 9, which aims to illustrate the used dimensions, where the inner dimension  $a = 14$  mm, the outer dimension  $b = 40$  mm, the flange dimension  $c = 90$  mm, and the waveguide length  $L = 95$  mm.

#### 2) AIR MEASUREMENT RESULTS

After the validation of the simulation results, we proceed in this part to the experimental measurement evaluation. Thus, we take the Air as a dielectric characterization benchmark. Note that the measured data are compared with HFSS-simulated data, which is obtained with the Air samples.

Figure 11(a) plots the transmission coefficient of the simulated result ( $Air_S$ ) against the measured result ( $Air_M$ ) for 10 mm of Air thickness simple. As we can clearly see from the figure, both curves have the same trend with a gap that depends on the frequency. This gap is due to the coaxial impedance deviation from the input impedance (i.e.  $50 \Omega$ ) to the output impedance (i.e.  $0.75 \Omega$ ) in the transition part of the real model. Hence, the ANN corrector bloc is introduced to reduce the gap between simulated and measured values.

Figure 12(a) represents the measured Air after correction ( $Air_C$ ). In this simulation, the mean-squared error (MSE) between the  $Air_S$  and the actual network outputs worth 0.29. At this point, the ANNs conversion can perfectly perform the dielectric material characterization.

#### 3) TEFLON MEASUREMENT RESULTS

After the validation of the ANNs corrector model, another experimental measurement evaluation is presented by taking the Teflon as a dielectric material benchmark. Note that the measured data are compared with HFSS-simulated data, which is obtained with Teflon samples.

Figure 11(b) plots the simulated transmission coefficient ( $Teflon_S$ ) against the measured transmission coefficient ( $Teflon_M$ ) for 10 mm of Teflon thickness simple.

Figure 12(b) represents the measured transmission coefficient of Teflon after correction ( $Teflon_C$ ). In this simulation, the MSE between the  $Teflon_S$  and the actual network outputs worth 0.33.

From Figs 11(a) and 11(b) we can clearly conclude that the shift between the simulated and measured depends crucially on the frequency as well as the material under test. As a result, the proposed ANNs corrector should be able to reduce the gap as much as possible between simulated and measured results.

In order to design and evaluate the ANNs corrector, 20 measurement samples are available. These samples are divided into a training set of ten measurements, a validation

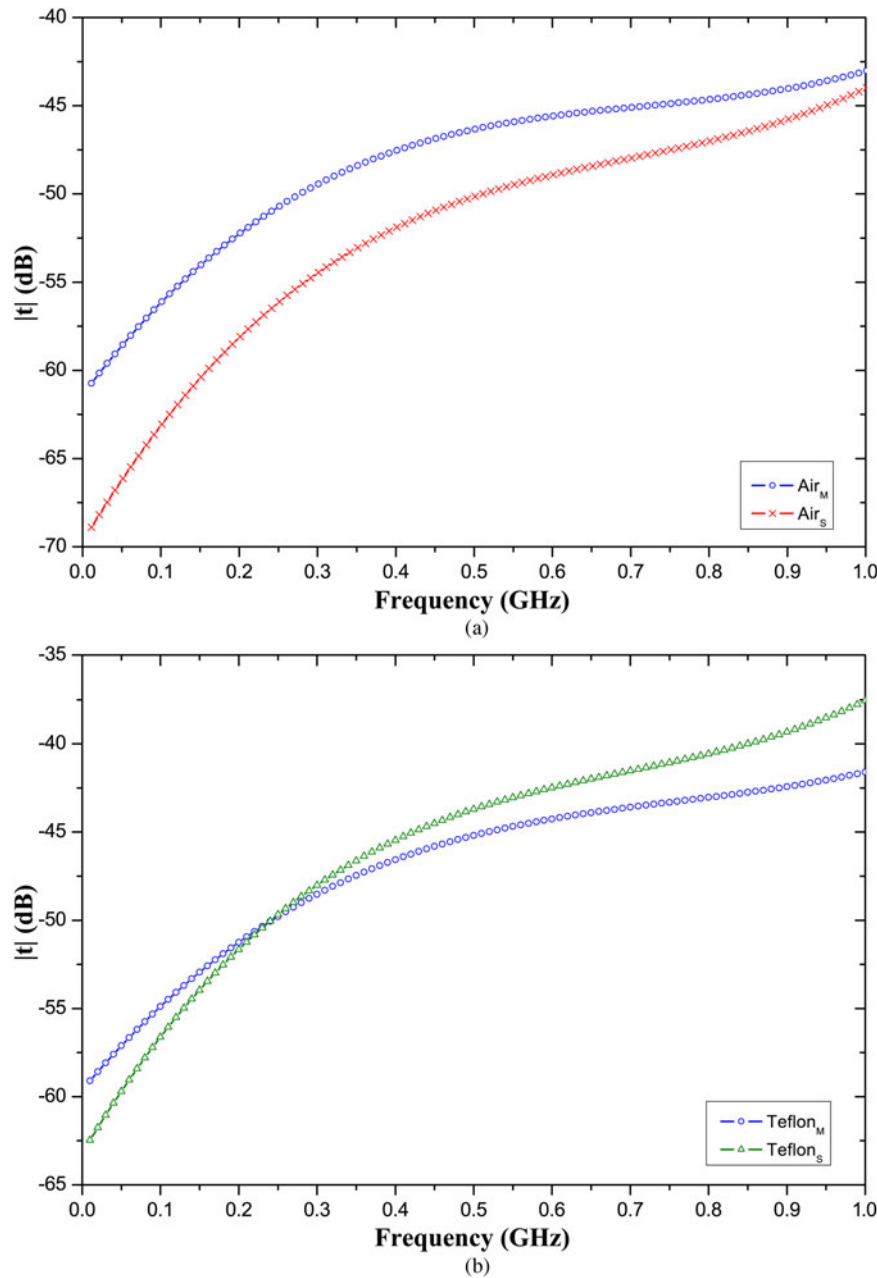


Fig. 11. Transmission coefficient comparison between measured and simulated data with 10 mm of thickness for (a) Air and (b) Teflon.

set of five measurements and a test set of five measurements. The weights are adjusted by using a gradient-descent error minimization technique. For this study the number of hidden layers and neurons are selected to minimize the error of the validation data.

As shown in Figs 12(a) and 12(b), the difference between the measured and simulated transmission coefficient become  $<0.5$  dB for both materials. These results confirm the ability of ANNs to solve the adaptation problem.

Table 2 summarizes the corrector testing performance for Teflon and Air.

At this stage, the conversion method leads to determine the dielectric coefficient of material under test.

The calibration part takes on consideration the real loss of the tester caused by the adaptation in the conical form, and the shift due to the reference plane and the air effect

on the measure. All those measures are introduced to the ANNs corrector to be considered during the conversion method.

## B) The evaluation of the conversion method

In this section, we evaluate the proposed conversion method. To this end, new data materials are introduced. The conversion method uses simulated samples with permittivity ranging from 1 to 81 and loss factor ranging from  $10^{-2}$  to 0. This range envelops all existing permittivity in the nature. In this work, we use some of them for the evaluation purposes.

In order to evaluate the performance of the conversion method, quantitatively, and verify whether there is any underlying trend in the performance, seven dielectric materials are considered. Note that this new variety of materials is not



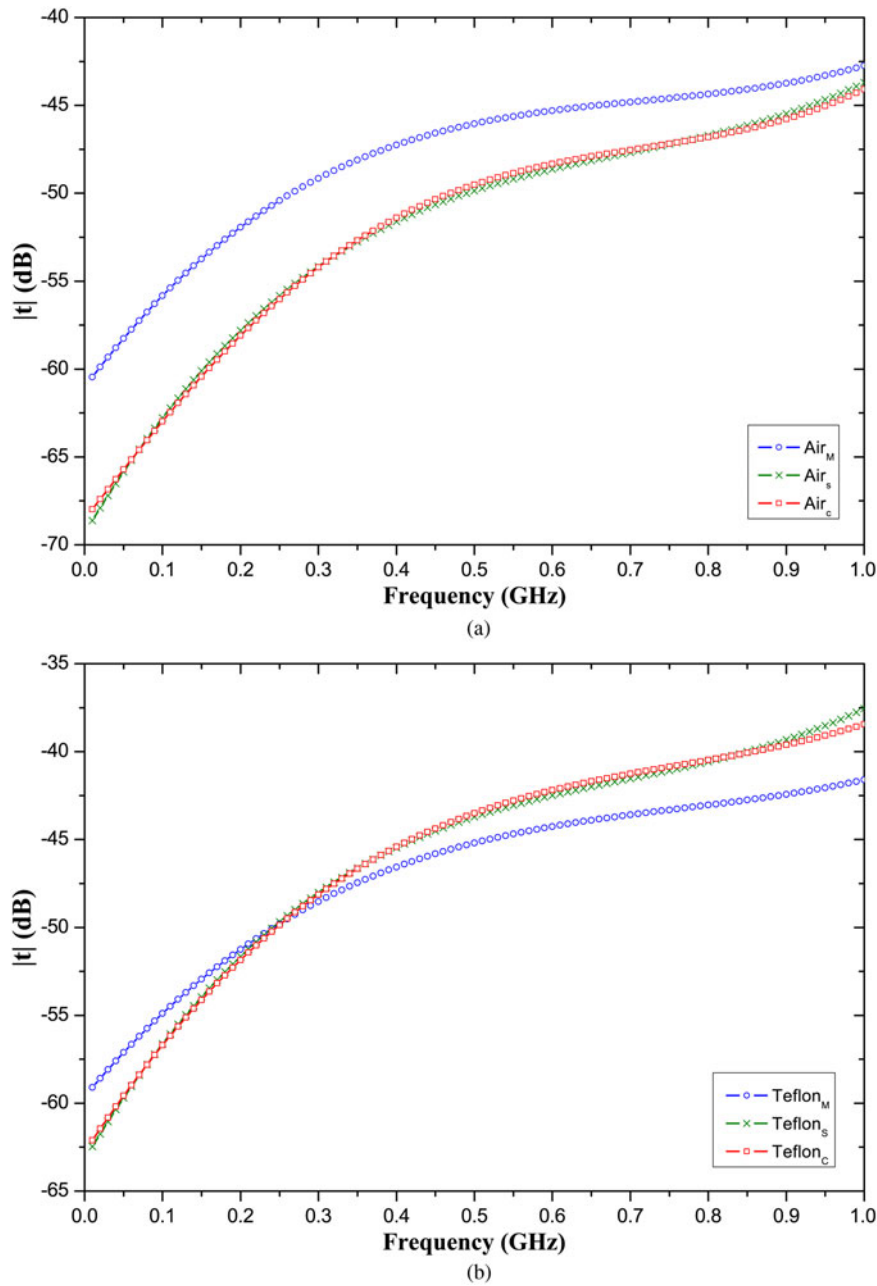


Fig. 12. Transmission coefficient comparison between measured, simulated and corrected by ANNs with 10 mm of thickness for (a) Air and (b) Teflon.

listed in our training database. Table 3 summarizes their permittivities and loss factors, obtained using ANNs and the benchmark [19]. Remember that the complex TR coefficients are the inputs and permittivity/loss factor are the outputs of the system. From Table 3, we can observe that the results obtained by the proposed method are very close to the results published in [19]. For instance, the comparison in terms of Air samples show  $\tilde{\epsilon}'_r = 0.9949$  and  $\tilde{\epsilon}''_r = 0.0058$ ,

which represents 0.57% of error. In addition, the comparison in terms of Teflon samples show  $\tilde{\epsilon}'_r = 2.0903$  and  $\tilde{\epsilon}''_r = 0.0014$ , which represents 0.46% of error. Regarding the loss factor,  $\tilde{\epsilon}''_r$ , its accuracy weakness is due to the small value and to its narrow distribution (i.e. from 0 to 0.01), whereas, since the permittivity values cover a large scale (i.e. from 1 to 81), it leads to better results. Therefore, the accuracy of ANNs is affected by the training sample distribution values.

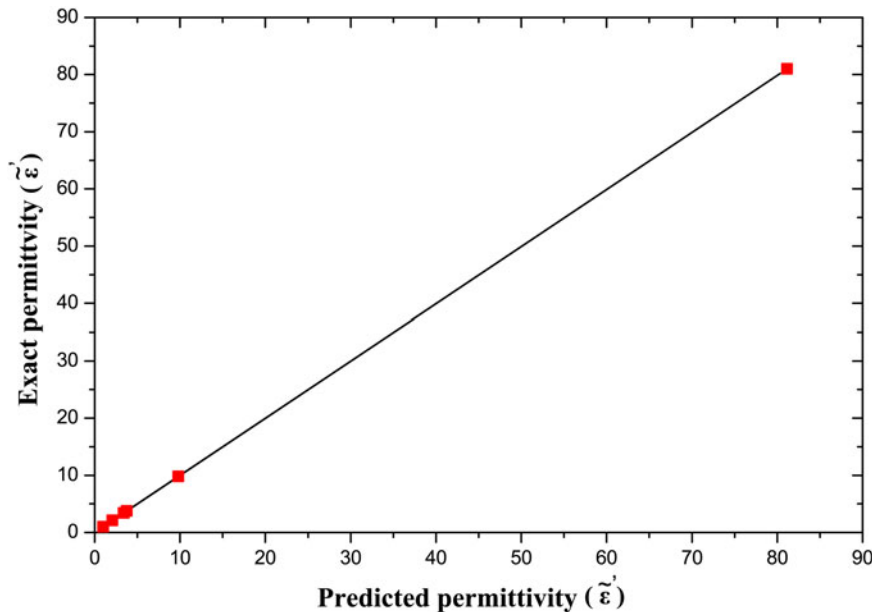
In Fig. 13, we present the interpolation of the predicted permittivity obtained by the ANNs against the exact permittivity. From the figure, we can observe a linear function, which confirms the stability of the conversion method. The presented result aims to show that the proposed method can predict a permittivity with lowest error regarding to the exact one.

Table 2 Corrector testing performance for Teflon and Air.

Material	Teflon	Air
MSE (dB)	0.33	0.29

**Table 3.** Dielectric results achieved at 1 GHz for 10 mm of thickness samples.

Dielectrics	Transmission coefficient		Reflection coefficient		ANN results		Published values	
	$ \tau $ (dB)	$\tau_\theta$ (°)	$ \rho $ (dB)	$\rho_\theta$ (°)	$\tilde{\epsilon}'_r$	$\tilde{\epsilon}''_r$	$\tilde{\epsilon}'_r$	$\tilde{\epsilon}''_r$
Plexiglas	-34.6145943	-171.9199364	-0.03222617	105.981768	3.4009	0.0096	3.4	0.001
Quartz	-33.73691	-173.7840603	-0.03524446	104.477748	3.7495	0.0598	3.78	0.0002
$AL_2O_3$ (ceramic)	-26.2621804	158.477325	-0.13631644	81.5821035	9.8098	0.0029	9.8	0.00214
Air	-44.791554	-158.8050766	-0.00504492	115.535521	0.9949	0.0058	1.0006	0
Vacuum	-44.7965607	-158.801372	-0.0050405	115.537966	0.9866	0.0017	1	0
Water	-23.722865	29.99895909	-0.48077038	-24.6047673	81.163	0.0094	81	0.0016
Teflon	-38.6147355	-165.1009402	-0.01618266	111.165293	2.0903	0.0014	2.1	0.001

**Fig. 13.** The interpolation of the exact permittivity versus the predicted permittivity.

## V. CONCLUSION

In this paper, a new conversion method based on the joint use of FEM and ANNs is presented. The proposed method aims to determine the dielectric characterization of the complex structure. During the experimental evaluation, a significant gap between the measured and simulated data is observed. This gap is caused by the conical form of the adopted structure. To overcome this issue, a concatenation of double stage of ANNs is proposed, where the first stage is designed to figure out the adaptation problem, whereas the second stage is used as a suitable conversion tool for the dielectric characterization.

It has been shown using experimental results, conducted on several materials, that the proposed system is efficient. Indeed, permittivity precision of 99.43 and 99.54% is achieved for Air and Teflon material, respectively.

As future work, the accuracy of the presented results could be improved via eliminating all air gap effects, increasing the number of training measured material and involving the high modes presented at the coaxial waveguide through exploring transversal operator method. Furthermore, the presented method can be extended to measure dielectric thicknesses and material identification.

## ACKNOWLEDGEMENT

The authors would like to thank Dr. H. Takhedmit from the University of Paris-Est Marne-la-Vallée for his valuable comments.

## REFERENCES

- [1] Cheng, G.; Liu, L.; Cai, D.; et al.: Microwave measurement of dielectric properties using the TM<sub>011</sub> and TE<sub>011</sub> modes excited by a generalized nonradiative dielectric resonator. *Meas. Sci. Technol.*, **23** (11) (2012), 115901–115912.
- [2] Kang, B.; Cho, J.; Cheon, C.; Kwon, Y.: Nondestructive measurement of complex permittivity and permeability using multilayered coplanar waveguide structures. *IEEE Microw. Wireless Compon. Lett.*, **15** (5) (2005), 381–382.
- [3] Hasar, U.C.: A fast and accurate amplitude-only transmission-reflection method for complex permittivity determination of lossy materials. *IEEE Trans. Microw. Theory Tech.*, **56** (9) (2008), 2129–2135.
- [4] Popovic, D. et al.: Precision open-ended coaxial probes for *in vivo* and *ex vivo* Spectroscopy of biological tissues at microwave

frequencies. *Trans. IEEE Microw. Theory Tech.*, MTT-53, 5 (2005), 1713–1721.

- [5] Muhamad, F.; Baba, N.H.; Awang, Z.; Ghodgaonkar, D.K.: Microwave non-destructive testing of semiconductor wafers in the frequency range 8–12.5 GHz, in *Proc. IEEE Int. Conf. Semiconductor Electronics*, 2002, 561–565.
- [6] Tamyis, N.; Ramli, A.; Ghodgaonkar, D.K.: Free space measurement of complex permittivity and complex permeability of magnetic materials using open circuit and short circuit method at microwave frequencies, in *IEEE Student Conf. on Research and Development*, 2002, 394–398.
- [7] Belenky, V.G. et al.: Accurate microwave resonant method for complex permittivity measurements of liquids. *IEEE Trans. Microw. Theory Techn.*, 48 (11) (2000), 2159–2164.
- [8] Luukkonen, O.; Maslovski, S.I.; Tretyakov, S.A.: A stepwise Nicolson–Ross–Weir-based material parameter extraction method. *IEEE Antennas Wireless Propag. Lett.*, (2011), 1295–1298.
- [9] De Paula, A.L.; Barroso, J.J.; Rezende, M.C.: Modified Nicolson–Ross–Weir (NRW) method to retrieve the constitutive parameters of low-loss materials, in *Microwave & Optoelectronics Conf.*, 2011, 488–492.
- [10] Hasar, U.C.: A microwave method for noniterative constitutive parameters determination of thin low-loss or lossy materials. *IEEE Trans. Microw. Theory Techn.*, 57 (6) (2009), 1595–1601.
- [11] Baker-Jarvis, J.; Janezic, M.; Grosvenor, J.; Geyer, R.: Transmission/reflection and short-circuit line methods for measuring permittivity and permeability, in *National Institute of Standards and Technology, Technical Note 1355-R*, 1993.
- [12] Scott, W.R.: A new technique for measuring the constitutive parameters of planar materials. *IEEE Trans. Instrum. Meas.*, 41 (5) (1992), 639–645.
- [13] Jin, J.: *The Finite Element Method in Electromagnetics*, 3rd ed., Wiley, Hoboken, NJ, USA, 2014.
- [14] Madenci, E.; Guven, I.: *The Finite Element Method and Application in Engineering Using ANSYS*, Springer International Publishing, 2015.
- [15] Bartley, P.G.; McClendon, R.W.; Nelson, S.O.: Permittivity determination by using an artificial neural network, in *IEEE Instruments and Measurement Technology Conf.*, 1999, 27–30.
- [16] Eugene, E.; Kopyt, E.P.; Yakovlev, V.V.: Determination of complex permittivity with neural networks and FDTD modeling. *Microw. Opt. Technol. Lett.*, 40 (3) (2004), 183–188.
- [17] Acikgoz, H.; Le Bihan, Y.; Meyer, O.; Pichon, L.: Microwave characterization of dielectric materials using bayesian neural networks. *Progress Electromagn. Res.*, 3 (2008), 169–182.
- [18] Mumbongo-Kambok, S. et al.: Original calibration method for dielectric property measurement cell of natural materials, in *Int. Conf. on Microwave and High Frequency Heating*, 2009.
- [19] Harrington, R.F.: *Time Harmonic Electromagnetic Fields*, McGraw-Hill, New York, 1961.



**Mohamed Mounkid Elafendi** was born in 1983 at Algiers, Algeria. He received the Dipl. Ing. degree in instrumentation engineering from the University of Science and Technology Houari Boumediene (USTHB), Bab Ezzouar, Algeria, in 2008. In 2009, he joined the laboratory of Instrumentation (LINS) in USTHB. He received the Magister degrees in 2011 on microwave for his study on waveguide radiation. From 2012 through 2015 he achieved technical training

during the summer in the Laplace laboratory of Toulouse (France). His field of interests are microwave theory, microwave non-destructive testing and applications and is currently working toward the Ph.D. degree.



**Mohamed Tellache** was born in Algeria in 1960. He received the Engineer degree in Electrical Engineering from the Ecole Nationale Polytechnique of Algiers in 1985. He received his Master degree in 1988 in Electronic Communication from Ottawa University, Canada and the Ph.D. degree in 2008 in Telecommunications from USTHB, Algeria. During

1995/1998, he spent 18 months at the Electronics Laboratory of INP-ENSEEIH, Toulouse, France, working principally on microwaves technology and modeling. He was the Head of the High School of Technology during 2009–2012 and before this, the Head of the Telecommunications Department in USTHB. Presently, he is an Associate Professor of Electrical Engineering at the faculty of Electronics and Computers of USTHB, working on the development of new algorithms for modeling microwave devices, numerical methods for electromagnetism, full wave characterization of microwave circuits, microwave and components design and communication systems.



**Junwu Tao** was born in Hubei, China, in 1962. He received the B.Sc. degree in Electronics from the University of Wuhan, China, in 1982; the Ph.D. degree from the INPT of Toulouse in 1988; and the Habilitation degree from the University of Savoie, in 1999. From 1983 to 1991, he was with the Electronics Laboratory of ENSEEIH, Toulouse,

where he was engaged in the application of numerical methods in electromagnetism, and the design of microwave and millimeter-wave devices. From 1991 to 2001, he was with the microwave laboratory, University of Savoie, where he was an Associate Professor in Electrical Engineering and was engaged in the full-wave characterization of discontinuity and the nonlinear transmission line design. Since September 2001, he has been a full Professor at the INPT, where he is engaged in the microwave and radio-frequency components design, millimeter-wave measurements, microwave material interaction, and research on microwave power applications.



**Bilal Hadjadj** was born in 1987 at Algiers, Algeria. He received his Master degree at the field of Electrical Engineering from the Faculty of Electronic and Computer Sciences, USTHB University, Algiers, Algeria, in 2012. Actually, he is a Ph.D. student in the same faculty. His research interests include machine learning, pattern recognition, one-class

classification, handwritten document analysis and recognition, classifier combination and image processing.



**Mouncef Benmimoune** received the Engineer and Magister degrees in Electronic Engineering from the USTHB, Algiers, Algeria, in 2006 and 2009, respectively, and Ph.D. degree in Electrical Engineering from the University of Quebec, Trois-Rivières, Canada, in 2013. During the summer of 2012, he

has been a visiting researcher at Imperial College London, Communication and Signal Processing

Group, London, UK. He held visiting scientist positions at Eurecom, Mobile Communications Group, Sophia Antipolis, France in 2013, and was with Laboratory of Signal and System Integrations from 2009 to 2013. Currently he is a Postdoctoral Research Fellow in TRIME Laboratory at the Department of Computer Engineering at the University of Quebec at Montreal in Canada. His current research interests include signal processing for wireless communications, multi-antennas communication systems, microwaves circuits, and hardware implementation issues.